Independent reflecting element interaction characterization for indoor visible light communication based on new generation lighting

Jupeng Ding (丁举鹏)*, Zhitong Huang (黄治同), and Yuefeng Ji (纪越峰)

Key Laboratory of Information Photonics and Optical Communications, Ministry of Education, Beijing University of Posts and Telecommunications, Beijing 100876, China

**E-mail: jupeng7778@163.com*

Received May 4, 2010

Indoor visible light communication (VLC) based on next generation environmentally friendly lighting is important in energy conservation. However, at present, the efficient characterization of VLC channels, including sophisticated reflection, has not yet been proposed. In this letter, we present a fast and comparably accurate channel characterization algorithm called independent reflecting element interaction characterization (IREIC), which can be used to describe optical power, illuminance, and impulse response.

OCIS codes: 230.3670, 200.2605, 200.2610.

doi: 10.3788/COL20100812.1182.

Optical data communication has been progressing from old wired networks based on fiber optics to wireless interconnection based on free space, such as visible light communication (VLC)[1−4]. The appearance and rapid advancement of VLC are inspired by multiple factors. First, solid state lighting technology has resulted in dramatic advances in increasing brightness, power conversion efficiency, and shortening the switching period. Second, the increasing demand in traditional radio frequency (RF) systems for high-speed analog-to-digital/digital-to-analog (AD/DA) conversion and complicated signal processing must be satisfied. In addition, a VLC system utilizing white light emitting diodes (WLEDs) can be used to implement indoor architectural lighting at the same time; this means that the development budget can be reduced substantially with the popularization of next generation environmentally friendly lighting[5−7].

In analyzing a VLC system, both the line of sight (LOS) link and the diffuse reflection link must be considered because the semi-angle of the WLED is much wider than that of laser diodes. Moreover, the adverse multipath dispersion at the receiving terminal is decided by reflection link to a large extent. To date, the efficient and specialized characterization of VLC channels, including sophisticated reflection, has not yet been proposed. For convenience, researchers have used infrared optical wireless modeling schemes as the base for characterizing VLC[8]. In practice, most of these models are time-consuming, crude, or restricted to impulse response analysis, and are unable to accurately depict the illuminance function analysis of VLC. For example, the channel response of the diffuse portion is approximated by an exponential function in Ref. [9]. This scheme has been adopted in Ref. [8] to estimate the channel gain of VLC. Although this approximation shortens the time needed for building the channel model in different indoor environments, the precision of the result is seriously affected because the gain of a diffused signal is viewed as a constant everywhere in a room. Mihaescu *et al.* have presented a physical method utilizing a reduced-size model to characterize the impulse response of the infrared optical wireless channel for simplifying analysis[10]. However, this method does not eliminate the time-consuming recursive calculation.

In this letter, a novel approach for the specialized efficient modeling of indoor VLC systems called independent reflecting element interaction characterization (IREIC) is proposed. This scheme classifies the modeling of diffuse links into three stages: 1) the characterization between the transmitters, i.e., WLED and the reflective elements; 2) the interaction between the reflective elements; 3) the general response of single or multiple receivers at the working level. This scheme makes full use of calculated interaction information between the fixed reflection elements and allows remarkable savings in computation time at the cost of limited permanent memory compared with existing unspecialized modeling schemes proposed for infrared optical wireless communication used in VLC for convenience. In addition, the scheme can be used to analyze the received optical power and illuminance, and is not restricted to impulse response.

The directed LOS link and the diffuse reflection links were conveniently classified according to the actual interaction between the transmitters and the receivers, as shown in Fig. 1. Given that the WLED transmitters have to provide illuminance simultaneously and the actual position of the receiver is not fixed, the semi-angle of the transmitter has to be wide enough to cover the entire working area. Moreover, the diffused reflection links are no longer negligible, which affects the received optical distribution, horizontal illuminance, delay spread, and so on. As such, we focused on the characterization of the reflection links and characterized this portion using an IREIC model.

As shown by the experimental measurements, many typical materials, such as plaster walls, have been well-approximated as Lambertian[11], and WLED has similar Lambertian radiation characteristic as well[12], in which

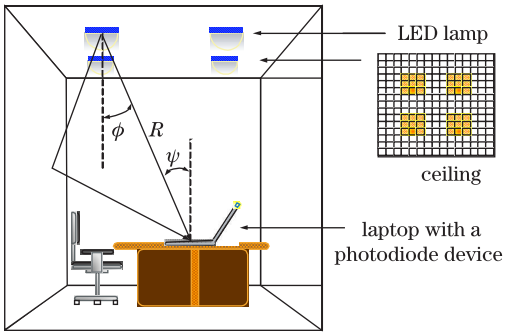

Fig. 1. Indoor VLC setup using directed LOS and diffuse reflection links. LED: light emitting diode.

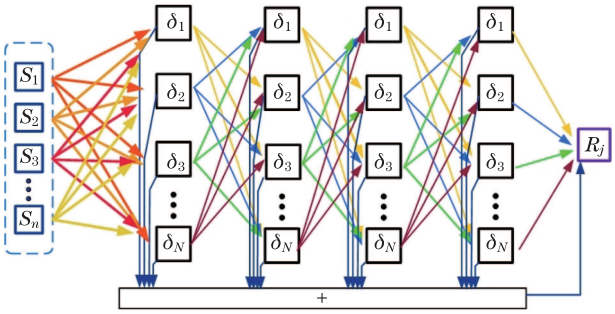

Fig. 2. Illustration of optical signal propagation using diffuse reflection. The indoor reflection surface is composed of N elements. The channel gain of any reflection is obtained by considering the elements within the FOV of the receiver. Each reflection causes N–1 reflections. Only the first to fourth reflections are presented.

the source and the reflection elements are assumed as pure generalized Lambertian emitters. Then, the six surrounding surfaces are divided into N differential reflecting elements. For a rectangular room with dimensions W, L, and M, the specific N is given as

$$N = 2\left(N_x N_y + N_x N_z + N_y N_z\right), \tag{1}$$

where $\frac{W}{N_x} = \frac{L}{N_y} = \frac{M}{N_z} = d$, and d represents the distance between the centers of the neighboring elements. For radiation undergoing $k \geq 1$ bounce, the channel gain at the receiver is given by

$$\mathbf{H}^k(S_i, R_j) = \sum_{l=1}^{N} \mathbf{H}^{(0)}(S_i, \delta_l) \cdot \mathbf{H}^{(k-1)}(\delta_l, R_j), \tag{2}$$

where S_i and R_j are the ith source and the jth receiver, respectively; δ_l is any of the reflective elements (Fig. 2).

Although traditional recursive methods can be used to analyze this problem, the computational time required for the calculation is prohibitive. Therefore, we propose a fast and comparably accurate channel characterization algorithm called IREIC to quantify the diffuse reflection channels of VLC.

The transmission between the source and the surface elements is accomplished. The transfer function can be expressed as an entry vector $\mathbf{H}_{\mathrm{Te}}$. Given that surface elements $1-N$ receive the signal directly, the gain of channel g_{Sk} between source S and element k is given by[13]

$$g_{Sk} = \frac{(m_{\mathrm{s}}+1)A_k}{2\pi R_{Sk}^2} \cos^{m_{\mathrm{s}}}(\phi_{Sk}) \cos(\psi_{Sk}) u\left(\frac{\pi}{2} - \psi_{Sk}\right), \tag{3}$$

where m_{s} is the Lambertian index of the source related to the transmitter semi-angle $\phi_{1/2}$ by $m_{\mathrm{s}} = -\ln 2/\ln[\cos(\phi_{1/2})]$; ϕ_{Sk} is the angle between a vectors perpendicular to S and a vector that originates from S and extends toward the kth element; ψ_{Sk} is the angle between a vector perpendicular to the kth element and a vector that lies on the straight line that connects S and the kth element; A_k is the receiving element area; R_{Sk} is the distance between source S and element k; function $u(\frac{\pi}{2} - \psi_{Sk})$ is the field of view (FOV) for each element, and is given by

$$u\left(\frac{\pi}{2} - \psi_{Sk}\right) = \begin{cases} 1 & \left(\frac{\pi}{2} - \psi_{Sk}\right) > 0 \\ 0 & \left(\frac{\pi}{2} - \psi_{Sk}\right) \leq 0 \end{cases}. \tag{4}$$

Therefore, for a single transmitter system, the vector $\mathbf{H}_{\mathrm{Te}}$ is expressed as

$$\mathbf{H}_{\mathrm{Te}} = [g_{\mathrm{T}1}\, g_{\mathrm{T}2} \ldots g_{\mathrm{T}k} \ldots g_{\mathrm{T}N}]. \tag{5}$$

This vector is shown as a block in Fig. 3.

The multiple-to-multiple interaction is inherently dependent on indoor geometry, dimensions, and reflective coefficients of each surface, and then the transfer function between any two reflecting elements is expressed. For description convenience, a matrix format is adopted and the order of reflections is up to n, which is used to account for the universality of this algorithm. It is expressed as

$$\mathbf{M}_n = \begin{cases} \mathbf{E}_{N\times N} + \mathbf{m} + \mathbf{m}^2 + \cdots + \mathbf{m}^{n-1} & n \geq 2 \\ \mathbf{E}_{N\times N} & n = 1 \end{cases}, \tag{6}$$

where $\mathbf{E}_{N\times N}$ is the $N \times N$ identity matrix, and $\mathbf{m}$ is presented by

$$\mathbf{m} = \begin{bmatrix} g_{11} & \cdots & g_{1N} \\ \vdots & \ddots & \vdots \\ g_{N1} & \cdots & g_{NN} \end{bmatrix}. \tag{7}$$

The entry g_{ij} is the channel gain between any two elements, i and j, and is expressed as

$$g_{ij} = \begin{cases} \frac{\rho_i (m_{\mathrm{e}}+1) A_j}{2\pi R_{ij}^2} \cos^{m_{\mathrm{e}}}(\phi_{ij}) \cos(\psi_{ij}) u\left(\frac{\pi}{2} - \psi_{ij}\right) & i \neq j \\ 0 & i = j \end{cases}, \tag{8}$$

where ρ_i is the reflection index of the ith element, and m_{e} is the Lambert index of the reflection element. This

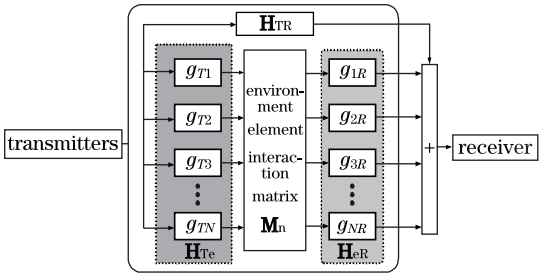

Fig. 3. New representation of VLC channel gain for multiple transmitters and a single receiver located at any position at the working level.

interaction matrix is independent of the source and the receiver; therefore, once obtained, it is suitable for any source/receiver configuration.

The transfer function between each reflection element and the receiver set at the working level is expressed as follows. This component is closely connected to the location information and FOV of the receivers. It is represented by matrix $\mathbf{H}_{\mathrm{eR}}$, which includes the gain of transmission between r receivers and N surface elements (Fig. 3). Specifically, it is given as

$$\mathbf{H}_{\mathrm{eR}} = \begin{bmatrix} g_{1R_1} & \cdots & g_{1R_r} \\ \vdots & \ddots & \vdots \\ g_{NR_1} & \cdots & g_{NR_r} \end{bmatrix}, \tag{9}$$

where g_{iR_j} can be calculated by

$$g_{iR_j} = \frac{\rho_i (m_{\mathrm{e}}+1) A_{R_j}}{2\pi R_{iR_j}^2} \cos^{m_{\mathrm{e}}}(\phi_{iR_j}) \cos(\psi_{iR_j}) \times u(\mathrm{FOV}_{R_j} - \psi_{iR_j}). \tag{10}$$

This number of $\mathbf{H}_{\mathrm{eR}}$ can illustrate symmetry if the receiver terminals of the same kind are placed uniformly in the working plane.

In the absence of reflections, the gain of the LOS channel can be expressed as

$$\mathbf{H}^{(0)} = \mathbf{H}_{\mathrm{TR}} = \left[g_{\mathrm{T}R_1} \cdots g_{\mathrm{T}R_r} \right]. \tag{11}$$

The entry g_{TR_i} accounts for the channel gain between the transmitter and the ith receiver and is expressed by

$$g_{\mathrm{T}R_i} = \frac{(m_{\mathrm{s}}+1) A_{R_i}}{2\pi R_{\mathrm{T}R_i}^2} \cos^{m_{\mathrm{s}}}(\phi_{\mathrm{T}R_i}) \cos(\psi_{\mathrm{T}R_i}) \times u(\mathrm{FOV}_{R_i} - \psi_{\mathrm{T}R_i}). \tag{12}$$

The directed LOS channel gain is represented by block $\mathbf{H}_{\mathrm{TR}}$ in Fig. 3.

The total channel gain $\mathbf{H}$ between a source and multiple receivers when n reflections are considered can be expressed as

$$\mathbf{H} = \sum_{i=0}^{n} \mathbf{H}^{(n)} = \mathbf{H}_{\mathrm{TR}} + \mathbf{H}_{\mathrm{Te}} \cdot \mathbf{M}_n \cdot \mathbf{H}_{\mathrm{eR}}. \tag{13}$$

$\mathbf{H}$ can be written as

$$\mathbf{H} = \mathbf{H}_{\mathrm{LOS}} + \mathbf{H}_{\mathrm{Reflection}}. \tag{14}$$

In an actual case, we are often interested in the channel gain for the many receiver locations or multiple receivers working simultaneously within a room. Generally, the parameters related to the room and the transmitters are relatively fixed in specific analysis, only parameters related to the receivers are variable. The time required for $\mathbf{H}_{\mathrm{Reflection}}$ is compatible with that required to calculate the total channel. Once $\mathbf{M}_n$ is calculated and stored, the time required to calculate a new total channel gain is reduced to the calculation of two matrices, a process that only takes a very short time to complete.

Table 1. Parameters

Height of Detector Surface (m)	0.85
Reflectivity of Ceiling	0.8
Reflectivity of Floor	0.3
Reflectivity of Surrounding Wall	0.8
Height of WLED Lights (m)	2.5
Transmitted Optical Power of WLED (mW)	63
Semi-Angle at Half-Power (deg.)	60
Maximum Luminous Intensity (cd)	9.5
Number of WLED in Four Lamps	900
Spacing of WLED in Each Lamp (cm)	7
FOV at Receiver (deg.)	60
Surface of PIN Photodiode (cm^2)	1
Area of Reflecting Elements on Ceiling/Floor (m^2)	0.25 × 0.25
Area of Reflecting Elements on Surrounding Four Surfaces (m^2)	0.25 × 0.15

PIN: positive intrinsic–negative.

We performed our simulation in an algorithm test room similar to configuration B in Ref. [8] with the following parameters: width $x = 5$ m, depth $y = 5$ m, and $z = 3$ m. Other important parameters related to this simulation are summarized in Table 1. The following simulation was realized utilizing MATLAB (7.10.0, R2010a).

The new algorithm makes it possible to obtain the received power for any order of reflections without extensive recursive calculations. Different from conventional radio systems, the input $X(t)$ of the VLC system must be non-negative. When $X(t)$ is given, the transmitted power P_{t} can be obtained according to a simple time-average relationship[13]. As the channel gain of our model has been identified, the received power can be expressed as

$$P_{\mathrm{r}} = \begin{cases} P_{\mathrm{t}} \left[\mathbf{H}_{\mathrm{TR}} + (\mathbf{H}_{\mathrm{Te}} \cdot \mathbf{M}_n \cdot \mathbf{H}_{\mathrm{eR}}) \right] & i \geq 0 \\ P_{\mathrm{t}} \mathbf{H}_{\mathrm{TR}} & i = 0 \end{cases}, \tag{15}$$

where i is the reflection order. The received optical power on the desk level is shown in Fig. 4. Figure 4(b) illustrates the corresponding optical power through the LOS link with a single-bounce reflection and adds the last power distribution at the edges of the working level to a certain extent. This case identifies that VLC has to make good use of the optical power through the reflection links, while considering that the available directed optical power is negligible close to the corners.

With the higher time reflection included, the received optical power increases steadily (Figs. 4(c) and (d)). Furthermore, we can observe that the ultimate optical power distribution is accompanied by obvious fluctuations in the area concerned (Fig. 4(d)).

Another measure of VLC system quality is the horizontal brightness on the working surface. When no reflection

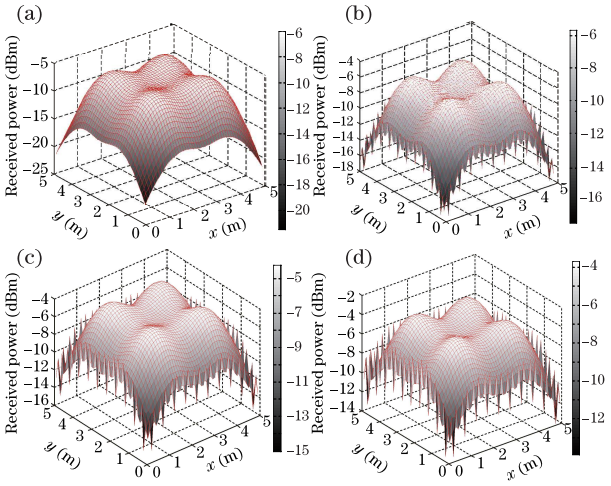

Fig. 4. Received optical power at the working level, (a) only through LOS, (b) through LOS with single-bounce reflection, (c) through LOS with up to double-bounce reflection, (d) through LOS with up to triple-bounce reflection.

is added, the horizontal illuminance is derived as

$$E_{\mathrm{h}} = I_0 \cos^{m_{\mathrm{s}}}(\phi)\cos(\psi)/R^2, \tag{16}$$

where $I_0 = I(\phi = 0)\Phi/2\pi$ is the center luminous intensity of the Lambert source, ϕ is the angle of irradiance, ψ is the angle of incidence, and R is the distance between the source and the receiver surface[14]. For estimating the effects of reflection on the total brightness distribution, the luminous flux of each reflective element has to be identified as a secondary source. The total luminous illuminance flux of each element can be calculated by

$$\Phi = \rho_{\mathrm{e}} E_{\mathrm{he}} A_{\mathrm{e}}, \tag{17}$$

where ρ_{e} is the reflective index of the reflective element, E_{he} is the surface brightness of the reflective element, and A_{e} is the area of the reflective surface element. According to Eq. (15), the surface brightness of the other element that receives illumination flux from the analyzed reflective element can be obtained.

Given that the illumination has been determined from a considerable part of the received optical power, which is sensitive to the eyes, the increase in horizontal illumination, including multiple reflections from one bounce to three bounces, conforms to that of the received optical power (Fig. 5). Furthermore, the eventual horizontal illumination is sufficient from 548.20 to 1222.71 lux by ISO at all locations within the room (Fig. 5(d)).

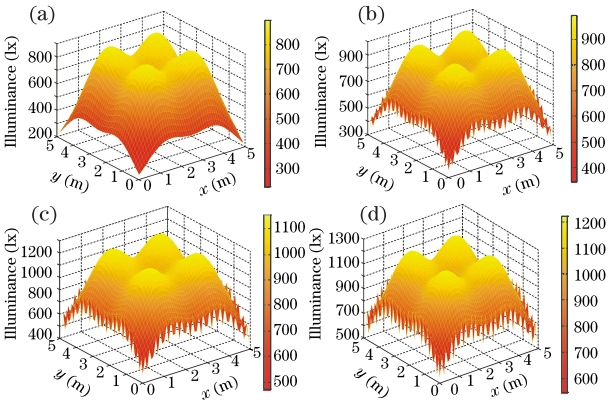

Fig. 5. Horizontal illuminance at the working level through (a) LOS, (b) LOS with single-bounce reflection, (c) LOS with up to double-bounce reflection, and (d) LOS with up to triple-bounces reflection.

The generally accepted recursive method proposed in Ref. [11] and the IREIC scheme were compared in order to evaluate fully the performance of the proposed IREIC algorithm. Figure 6 shows the simulated impulse response results for the configuration A depicted in Ref. [11]. The utilized simulation environment was MATLAB using an Intel (R) Core (TM) 2 Duo CPU E7500 processor.

Figure 6(a) presents the impulse response obtained from the recursive method. Reflections of up to 3 bounces were concluded in this total impulse response. The time resolution is 0.2 ns, which is the bin width of the power histogram that approximates the impulse response; the spatial resolution of the simulation is 100 for the single-bounce reflection, 20 for the double-bounce reflection, and 5 for the triple-bounce reflection, as specified by the number of partitions per meter. All of these parameters are consistent with their counterparts in configuration A shown in Ref. [11]. The LOS impulse response is an isolated delta peak; the sum of the reflection impulse responses has 4 peaks that exactly reappear as the character depicted in Ref. [11] (Fig. 6(a)). According to our actual measurements, the time required to obtain Fig. 6(a) is roughly 67 h.

The impulse response for the receiver located at the same position utilizing the IREIC scheme is plotted in Fig. 6(b). To keep in step with the check simulation in the parameters, we utilized the set of time solution that has been applied to depict Fig. 6(a) and set the spatial solution with 100 partitions per meter for the single-bounce reflection, 10 partitions per meter for the double-bounce reflection, and 5 partitions per meter for the triple-bounce reflection considering the maximum matrix size supported by MATLAB. By observation, the agreement between Figs. 6(a) and (b) is satisfactory; therefore, the accuracy of IREIC is proven to a great extent. Apart from this, the simulation reveals the potential of the IREIC scheme compared with the generally accepted recursive method. Furthermore, the corresponding experimental measurement shows that the average simulation time is less than 5.3 h when considering up to the 3-rd order reflections. The figure illustrates the temporal dispersion and the magnitude variance of the response undergoing increased reflection.

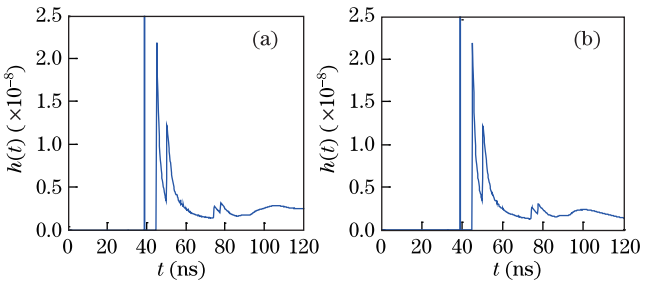

Fig. 6. Impulse response results for the receiver located at (0.5, 1.0, 0) (for configuration A, assuming a source power of 1 W[11]) obtained through (a) the recursive method and (b) the IREIC scheme.

In conclusion, the characterization of a new indoor VLC based on new generation lighting equipment is proposed. This mechanism for channel model analysis avoids the extensive recursive calculations used in existing approaches. The received optical power distribution, illumination, and impulse response are generated. With accuracy, the time required to accomplish the simulation of impulse response based on the IREIC scheme is quite less than its counterpart, based on the generally accepted recursive method; it also demonstrates the superiority of this novel analysis approach over other existing recursive methods.

This work was supported in part by the National "863" Program of China (No. 2009AA01A345), the National Natural Science Foundation of China (No. 60932004), the National "973" Program of China (No. 2007CB310705), and the Chinese Universities Scientific Fund (No. BUPT2009RC0126).

References

1. H. Elgala, R. Mesleh, and H. Haas, IEEE Trans. Consum. Electron. **55,** 1127 (2009).
2. H. Wang and X. Ke, Acta Opt. Sin. (in Chinese) **29,** 132 (2009).
3. Y. Wang, L. Yu, and J. Cao, Acta Opt. Sin. (in Chinese) **29,** 3295 (2009).
4. S. K. Hashemi, Z. Ghassemlooy, L. Chao, and D. Benhaddou, in *Proceedings of IEEE CSNDSP08* 174 (2008).
5. Nichia: http://www.nichia.com/.
6. Lumileds: http://www.philipslumileds.com/.
7. Osram: http://www.osram.cz/osram_cz/.
8. J. Grubor, S. Randel, K.-D. Langer, and J. W. Walewski, J. Lightwave Technol. **26,** 3883 (2008).
9. V. Jungnickel, V. Pohl, S. Nönning, and C. von Helmolt, IEEE J. Sel. Areas Commun. **20,** 631 (2002).
10. A. Mihaescu, A. Songue, P. Besnard, O. Bouchet, and Q. Liu, in *Proceedings of IEEE CSNDSP08* 544 (2008).
11. J. R. Barry, J. M. Kahn, W. J. Krause, E. A. Lee, and D. G. Messerschmitt, IEEE J. Sel. Areas Commun. **11,** 367 (1993).
12. T. Komine, J. H. Lee, S. Haruyama, and M. Nakagawa, IEEE Trans. Wireless Commun. **8,** 2892 (2009).
13. J. M. Kahn and J. R. Barry, Proc. IEEE **85,** 265 (1997).
14. T. Komine and M. Nakagawa, IEEE Trans. Consum. Electron. **50,** 100 (2004).